Volume 1 | Number 1 | Jan 2013 | Pages 1–100

Journal of
Materials Chemistry C

Materials for optical and electronic devices
www.rsc.org/materialsC

ROYAL SOCIETY
OF CHEMISTRY

ROYAL SOCIETY
OF CHEMISTRY

www.rsc.org/materialsC

Journal Name

Dynamic Article Links ▶

ARTICLE TYPE

CEE-Active Red/Near-Infrared Fluorophores with Triple-Channel Solid-State "ON/OFF" Fluorescent Switching

Xiao Cheng, Zhenyu Zhang, Houyu Zhang, Shenghua Han, Kaiqi Ye, Lu Wang, Hongyu Zhang* and Yue Wang

A class of beryllium complexes has been synthesized. These complexes display crystalline-enhanced emissions (CEE) and exhibit morphology-dependent dark and bright red/NIR fluorescence. They show bright red/NIR emissions in the crystalline form (λ_{em}: 635–700 nm; Φ_f: 0.27–0.40) and faint emissions in
10 amorphous state. Their emissions can be smoothly switched "ON" and "OFF" by simple grinding/solvent annealing processes. In addition, these complexes show interesting acid/base vapor induced fluorescent switching properties due to the amino groups of the ligands. Furthermore, the molecular packing modes of these complexes can be altered by heating and recovered by solvent annealing accompanied with fluorescence switching between dark and bright states. The first example of reversible triple-channel
15 solid-state fluorescent "ON/OFF" switching realized through simple approaches of grinding/solvent annealing, acid/base vapor fuming, and heating/solvent annealing might have great significance on designing novel organic materials as chemical sensors.

1. Introduction

The molecular design and construction of organic/organometallic
20 materials exhibiting highly efficient luminescence in the solid state have increasingly attracted much attention because of their applications in solid-state lasers, chemical sensors, and organic light-emitting diodes.[1,2] Among those, materials possessing switchable emissions have been considered as candidates for
25 optical data storage and sensors. Thus, an important issue regarding luminescent materials is how to effectively tune their solid-state emission colors or achieve reversible fluorescence switching between dark/bright states. Recent achievements have demonstrated that the molecular conformation or packing mode
30 plays an important role in modulating the luminescent properties of organic materials in the solid state.[3] Therefore, manipulating the molecular conformation or packing manner of the organic materials might serve as an effective approach to tune their solid-state emissions. Indeed, different emission colors or efficiencies
35 based on a single fluorophore have been achieved by externally stimulating the solid sample.[4−6] Switchable solid-state emissions based on a single fluorophore are possible to be achieved by external stimuli such as pressure, vapor, light, heat, and acid etc. Indeed, a lot of stimuli-responsive organic fluorophores with
40 tunable emission colors have been constructed and some of them even display fluorescence switching among three or four distinctly different colors.[7] However, most of these smart materials reported so far are mainly focused on solid-state emission color change, and the controllable fluorescence
45 "ON/OFF" switching with high contrast ratio is very limited.[8] Particularly, the luminescent materials with reversible fluorescent

"ON/OFF" switching which can be realized by three or more different procedures has never been reported. Therefore, multiple-channel reversible "ON/OFF" fluorescence switching of organic
50 solids (depicted in Chart 1) is considered to be an uncovered but highly important research topic and thus is well worth exploring.

We recently synthesized 2'-hydroxychalcone chelated boron and beryllium complexes with morphology-dependent emission intensity and found the boron species displayed a dual-channel
55 solid-state fluorescence switching.[9] These findings encourage us to attempt the possibility of realizing multiple-channel solid-state "ON/OFF" fluorescent switching. In this contribution, we newly synthesized four beryllium complexes **2−5** (Scheme 1) and subsequently focused the point on their fluorescence switching
60 behaviors including the previous complex **1** under different external stimuli. All the complexes are highly red or NIR fluorescent in the crystalline state while they are faintly emissive in solutions and amorphous films, showing a typical crystalline-enhanced emission (CEE) feature.[10] The morphology-dependent
65 emission intensity and acid-responsive property of these materials allow the first realization of a triple-channel fluorescence switching between "ON" and "OFF" states based on different mechanisms.
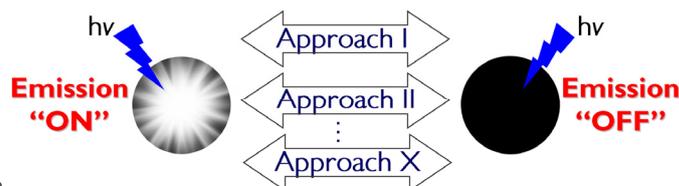
70 **Chart 1.** Schematic of multiple-channel ON/OFF fluorescence switching.

Journal of Materials Chemistry C Accepted Manuscript
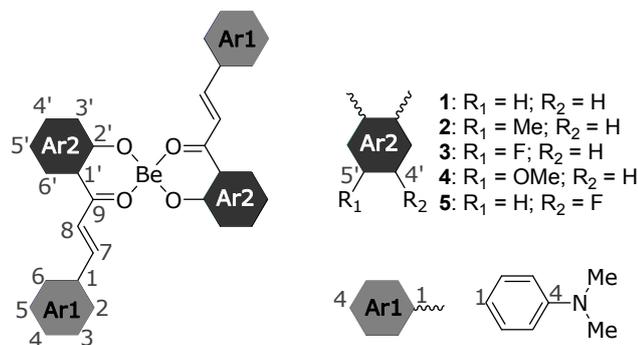
Scheme 1. Molecular structures of complexes **1**–**5**.

2. Experimental section

2.1 Materials

All starting materials were purchased from Aldrich Chemical Co. and used without further purification. The solvents for syntheses were common commercial grade and were used as received.

2.2 Instrumentation

NMR spectra were recorded on a Bruker AVANCE 300 or 500 MHz spectrometer with tetramethylsilane as the internal standard. Mass spectrum was recorded on a GC/MS mass spectrometer. Element analyses were performed on a FlashEA1112 spectrometer. UV−vis absorption spectra were recorded by a Shimadzu UV-2550 spectrophotometer. The emission spectra of solutions were recorded by a Shimadzu RF-5301 PC spectrometer. The emission spectra of crystals/powders were recorded using a Maya2000 Pro CCD spectrometer. The absolute fluorescence quantum yields were measured on Edinburgh FLS920 in an integrating sphere. Thin film/Powder X-ray diffraction data were collected at 298K on a Bruker SMART-CCD diffractometer. Differential scanning calorimetric (DSC) measurements were performed on a NETZSCH DSC204 instrument.

2.3 Computational details

Ab initio calculations were carried out with the Gaussian 09 program. Geometry at ground state was optimized with the density functional theory (DFT) using the B3LYP functional and 6–31G** basis set. The geometry optimization at excited state and vertical transitions were performed with the time–dependent density functional theory (TDDFT) at the same level of theory.

2.4 Single crystal structure

Single crystal X-ray diffraction data were collected on a Rigaku RAXIS-PRID diffractometer using the ω-scan mode with graphite-monochromator Mo Kα radiation. The structures were solved with direct methods using the SHELXTL programs and refined with full-matrix leastsquares on F^2. Non-hydrogen atoms were refined anisotropically. The positions of hydrogen atoms were calculated and refined isotropically.

2.5 General synthetic procedure

In a 100 mL round-bottomed flask, a mixture of 1.0 mol derivatives of 2'-hydroxychalcone and 1.0 mol sodium hydroxide dissolved in MeOH was heated to reflux. Then a solution of 0.5 mol beryllium sulfate in water was added and the mixture was

refluxed for 24 h. After cooling, the produced precipitates were filtered. The solid was recrystallized twice from CH_2Cl_2/MeOH 1:2 to yield the pure beryllium complex.

Complex 2. Yield: 80%. ^{1}H NMR (CDCl$_3$, 500 MHz, ppm): δ 8.06 (d, J = 15 Hz, 1 H), 7.80 (d, J = 8.5 Hz, 1 H), 7.54 (d, J = 9.0 Hz, 2 H), 7.50 (d, J = 15 Hz, 1 H), 6.81 (s, 1 H), 6.67 (d, J = 9.0 Hz, 2 H), 6.52 (dd, J = 8.5 Hz, 1.5 Hz, 1 H), 3.04 (s, 6 H), 2.31 (s, 3 H). ^{13}C NMR (125 MHz, CDCl$_3$): δ 188.55, 170.57, 152.40, 149.68, 148.03, 131.19, 129.96, 123.63, 118.63, 117.43, 114.11, 111.94, 40.25, 22.29. MS m/z: 569.86 [M]$^+$ (calcd: 569.28). Anal. Calcd (%) for C$_{36}$H$_{36}$BeN$_2$O$_4$: C, 75.90; H, 6.37; N, 4.92; Found: C, 74.98; H, 6.30; N, 4.95.

Complex 3. Yield: 84%. ^{1}H NMR (CDCl$_3$, 300 MHz, ppm): δ 8.10 (d, J = 15 Hz, 1 H), 7.94 (dd, J = 9.3 Hz, 7.2 Hz, 1 H), 7.56 (d, J = 9.0 Hz, 2 H), 7.44 (d, J = 12 Hz, 1 H), 6.65 (m, 3 H), 6.46 (m, 1 H), 3.06 (s, 6 H). MS m/z: 577.77 [M]$^+$ (calcd: 577.23). Anal. Calcd (%) for C$_{34}$H$_{30}$BeF$_2$N$_2$O$_4$: C, 70.70; H, 5.24; N, 4.85; Found: C, 69.60; H, 5.12; N, 4.76.

Complex 4. Yield: 85%. ^{1}H NMR (CDCl$_3$, 300 MHz, ppm): δ 8.05 (d, J = 15 Hz, 1 H), 7.84 (d, J = 12 Hz, 1 H), 7.56 (d, J = 8.7 Hz, 2 H), 7.46 (d, J = 15.3 Hz, 1 H), 7.01 (d, J = 8.4 Hz, 2 H), 6.45 (d, J = 2.4 Hz, 1 H), 6.33 (dd, J = 9.0 Hz, 2.4 Hz, 1 H), 3.82 (s, 3 H), 3.05 (s, 6 H). MS m/z: 601.84 [M]$^+$ (calcd: 601.27). Anal. Calcd (%) for C$_{36}$H$_{36}$BeN$_2$O$_3$: C, 71.86; H, 6.03; N, 4.66; Found: C, 70.89; H, 6.09; N, 4.71.

Complex 5. Yield: 86%. ^{1}H NMR (CDCl$_3$, 500 MHz, ppm): δ 8.13 (d, J = 14.5 Hz, 1 H), 7.57 (m, 3 H), 7.40 (d, J = 15 Hz, 3 H), 7.23 (d, J = 3.0 Hz, 1 H), 6.97 (dd, J = 9.0 Hz, 4.5 Hz, 1 H), 6.75 (s, 2 H), 3.08 (s, 6 H). MS m/z: 577.94 [M]$^+$ (calcd: 577.23). Anal. Calcd (%) for C$_{34}$H$_{30}$BeF$_2$N$_2$O$_4$: C, 70.70; H, 5.24; N, 4.85; Found: C, 69.73; H, 5.17; N, 4.74.

3. Results and discussion

3.1 Optical properties in various states
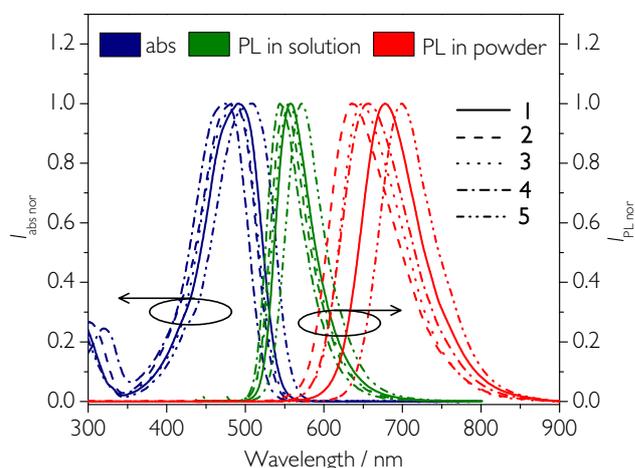
Figure 1. Absorption and emission spectra of beryllium complexes **1**–**5** in CH_2Cl_2.

The optical properties of **1**–**5** in CH_2Cl_2 (concentration: 1×10^{-5} M) were carried out (Figure 1) and their data are summarized in Table 1. Complex **1** shows a strong absorption band centered at 490 nm, corresponding to the π→π* transition of the molecule. The absorption bands of **2** and **3** are slightly blue shifted by 3 and

6 nm, respectively, compared to that of complex **1**. This comparison reflects that the fluoro atom or methyl group at the 4'-position on the ligand don't greatly affect the optical gap of this type of Be(II) complex. 4'-Methoxyl group substituted complex **4** shows the strongest absorption band at 472 nm which is blue shifted by 18 nm compared to that of **1**, reflecting that introducing electron-donating group on the ligand has a considerable effect on the absorption properties of the formed complex. Notably, complex **5** with fluoro atom substituted at 5'-position displays quite different absorption behaviors compared to its analog 4'-fluoro substituted **3**. In comparison with complex **1**, the absorption band of **3** is slightly blue-shifted by 3 nm while that of **5** is greatly red-shifted by 18 nm, demonstrating that the substitution position also has certain effect on the optical properties of the beryllium complexes.
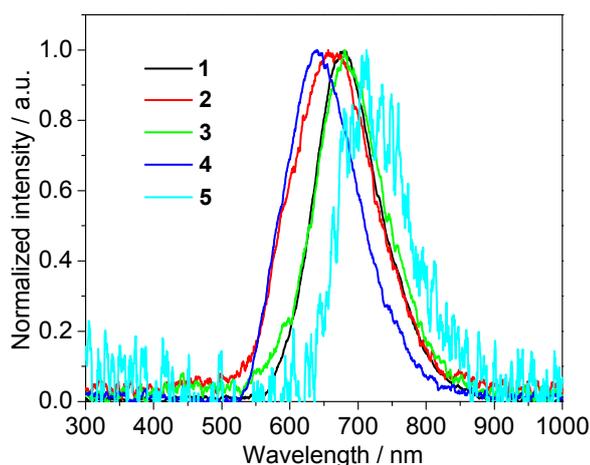
Figure 2. Photoluminescent spectra of complexes **1**–**5** in amorphous states.

Complex **1** is yellow luminescent with an emission band peaking at 557 nm. The photoluminescent (PL) spectra of complexes **1**–**5** display the same substitution effects as the absorption spectra. The methyl and fluoro substituted complexes **2** and **3** slightly blue-shift the emission peak from 557 nm to 555 and 550 nm, respectively. The electron-donating methoxy group substituted complex **4** is green emissive with an emission peak at 543 nm, which is blue shifted by 14 nm compared to that of **1**. The 5'-fluoro substituted complex **5** displays orange fluorescence which is red-shifted by 20 nm compared to its 4'-fluoro substituted ananlog **3**. The quantum yields (Φ_f) of these complexes in CH_2Cl_2 (1×10^{-5} M) determined by an integrating sphere are 0.10 for **1**, 0.09 for **2**, 0.03 for **3**, 0.15 for **4**, and 0.01 for **5**. The relatively low Φ_f suggests that these complexes are not efficient emitters in solutions. TD-DFT calculations have been performed for complex **1** to reveal the emission process for these complexes. For the emission process, the electronic transition between S_1 and S_0 is forbidden. The emission peak originated from the excited state S_3 is around 525 nm, which is in agreement with the experimental value of 557 nm in CH_2Cl_2 solution. The frontier orbitals involved in the emission process are featured with their electron density partially located in either one ligand or part of the complex (as shown in Figure S1). This might be ascribed to the distorted excited state structure of the complex.

Table 1 Optical data of complexes **1**–**5** in different phases

complex	λ_{abs}/nm[a]	λ_{em}/nm(Φ, τ/ns)[b]	λ_{em}/nm(Φ, τ/ns)[c]	λ_{em}/nm(Φ)[d]
1	490	557(0.10, 0.31)	678(0.27, 2.11)	678(<0.01)
2	487	555(0.09, 0.55)	635(0.33, 2.12)	656(<0.01)
3	484	550(0.03, 0.23)	648(0.40, 2.35)	680(<0.01)
4	472	543(0.15, 0.42)	658(0.30, 1.68)	639(<0.01)
5	508	570(0.01, 0.18)	700(0.31, 1.75)	710(<0.01)

[a] in CH_2Cl_2 solution (1×10^{-5} M), [b] in CH_2Cl_2 solution (1×10^{-5} M), [c] in crystalline state, [d] in amorphous state.

The fluorescence color and efficiency of these complexes in the solid state are quite different to those of solutions. The PL spectra of the solid powders (Figure 1) are all greatly red-shifted compared to those of solutions due to the aggregation effects (Table 1). The powder of **1** exhibits deep red fluorescence at 678 nm, which is red-shifted by 121 nm compared to that of **1** in CH_2Cl_2 (557 nm). Complexes **2**–**4** are all brightly red fluorescent with the emission maxima at 635, 648 and 658 nm, respectively, and complex **5** displays NIR emission at 700 nm. For most of the red/NIR emitters, their Φ_f will be inevitably reduced after they aggregate from dispersed states into solids. However, the Φ_f of powders are 0.27 for **1**, 0.33 for **2**, 0.40 for **3**, 0.30 for **4** and 0.31 for **5**, significantly higher than those of their solutions (0.10 for **1**, 0.09 for **2**, 0.03 for **3**, 0.15 for **4**, and 0.01 for **5**), displaying a typical crystalline-enhanced emission feature. The fluorescence lifetime of the solution are shorter than those of the crystals, consistent with their emission behavior. In sharp contrast to the high efficiency of complexes **1**–**5** in the crystalline state, the spin-coating thin films which are amorphous in nature as demonstrated by PXRD show very weak red/NIR emissions (Φ_f<0.01, Table 1 and Figure 2). Thus, these beryllium complexes display morphology-dependent emissions which make them to be possible candidates for fluorescent "ON/OFF" switching.
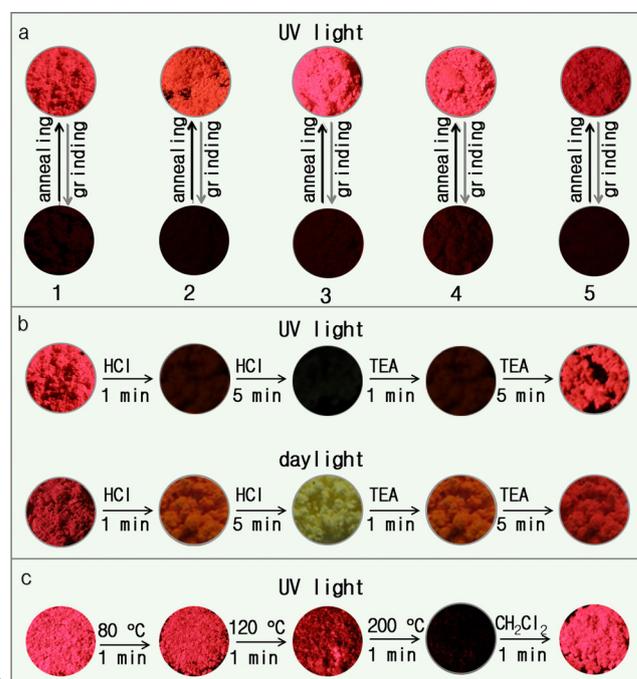
Figure 3. Photographic images showing fluorescent dark and bright states switched by different processes: a) grinding and solvent annealing of **1**–**5**; b) protonation/deprotonation and c) heating and solvent annealing of **4**.

3.2 Solid-state "ON/OFF" fluorescent switching

The aggregation modes of **1–5** in solid forms can be readily interconverted between crystalline and amorphous states by very simple engineering processes: mechanical grinding and solvent annealing. The emission intensities of the ground samples are significantly reduced compared to those of the crystalline samples, indicating the fluorescence is turned "OFF" (Figures 3a, 4a and 5). PXRD patterns show strong signals for the unground powders but very weak diffraction peaks for the ground sample, demonstrating the morphology conversion from crystalline form to amorphous state after mechanical grinding (Figure S2). The dark samples can revert to another crystalline state as demonstrated by PXRD patterns and the emission intensities perfectly restore (turn "ON") after annealing by CH_2Cl_2 atmosphere within 1 min in a closed container. This reversible fluorescent "ON/OFF" switching by grinding/annealing operation can be repeated with no fatigue and loss of the emission intensity (Figure 4a).
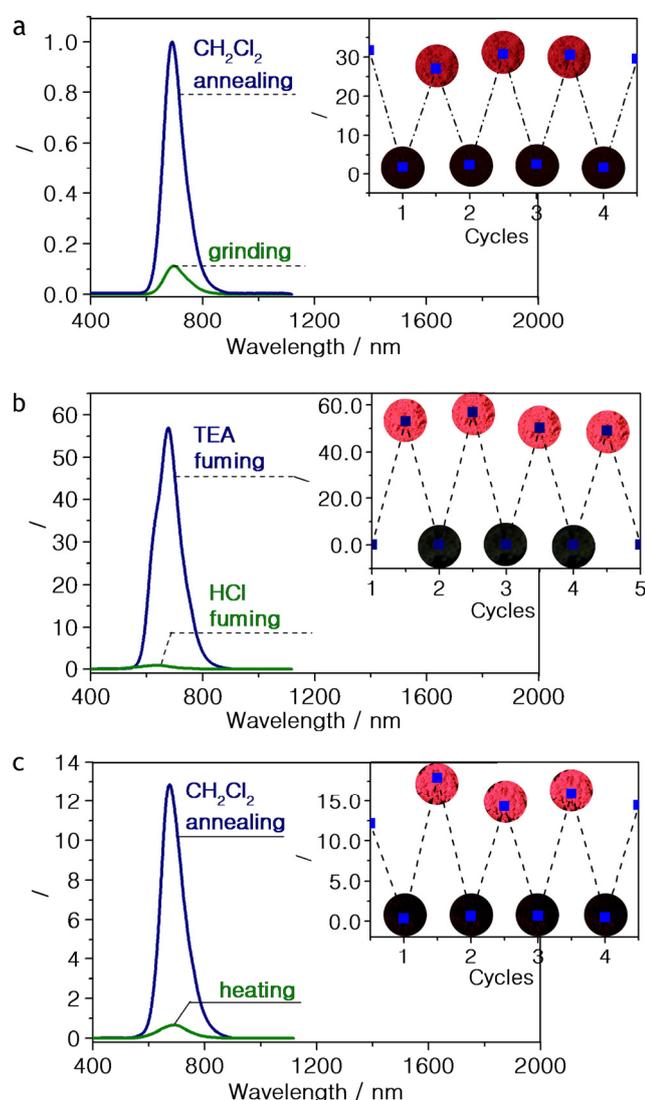
Figure 4. Fluorescence "ON/OFF" switching of **4** realized by a) grinding/annealing process; b) acid/base vapor fuming process and c) heating/annealing process (inset: repeated switching between dark and bright states of the solids).
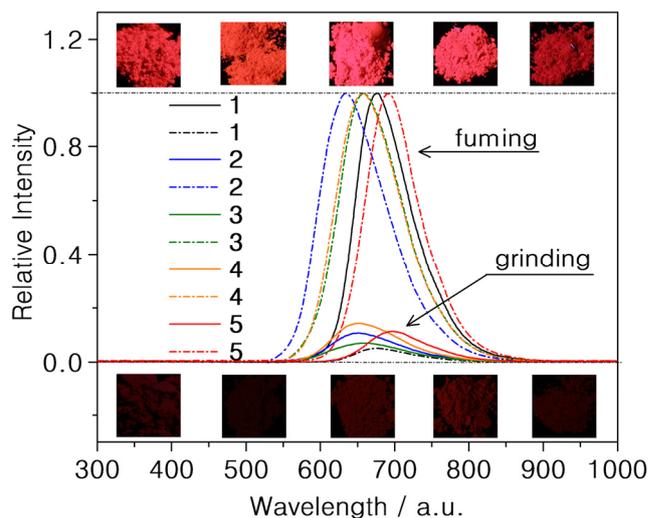
Figure 5. Photoluminescent spectra of ground and fumed samples of complexes **1–5**.

The fluorescence of solids **1–5** is in response to hydrochloride acid (HCl) vapor due to the Lewis-base nature of nitrogen atoms in amino groups (Figure 4b). For example, after evaporated by HCl vapor for several seconds, the red sample of **4** converted into an orange solid accompanied with fluorescence changing from deep red to orangered ($658 \rightarrow 630$ nm) accompanied with emission intensity decreasing, likely owing to the protonation of one amino group (Figure S3). The blue-shift of the emission band is due to the diminished intramolecular charge-transfer transition (Figures 6 and S4). And the quenched emission is probably because of the changed molecular conformation and packing structure (Figure S5). The orange sample was further converted into an yellow-colored solid and displayed almost no fluorescence (λ_{em} = 574 nm) after fuming by HCl vapor for another 5 min, due to the further protonation of the other amino group. The yellow sample gradually recovered its original red color and fluorescence through an orange intermediate state when it was treated with triethylamine (TEA) vapor for several minutes. The contrast ratios I_{on}/I_{off} for **1–5** are 100, 16, 43, 62 and 75, respectively (Figure S6). The switching between fluorescence "OFF" and "ON" states by acid/base vapor fuming can be carried out repeatedly without obvious intensity decaying (Figure 4b).
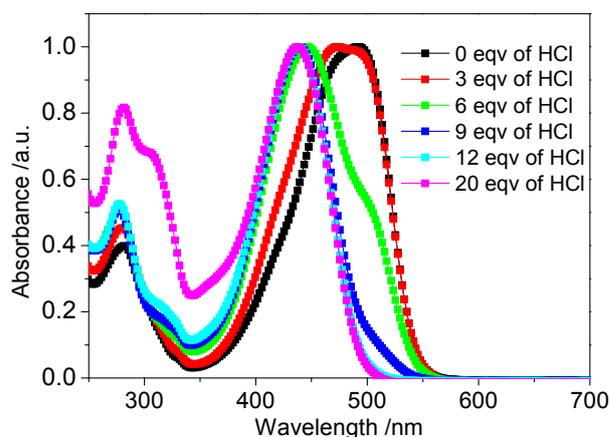
Figure 6. Absorption spectra of complex 1 acidized with HCl.

It is interesting to point out that the beryllium solids exhibit heating-induced phase transformation together with reversible fluorescent "ON/OFF" switching (Figures 4c and S7). For instance, when the crystalline sample **4** was heated to 240 °C, the deep red emission gradually faded away and the sample converted to a non-luminous red solid ($I_{ON}/I_{OFF} = 22$). The heated sample recovered one-third of fluorescence by cooling to room temperature while perfectly reverted to the red luminescence by immediate CH_2Cl_2 vapor annealing. The reversible thermal and annealing cycles demonstrate that this fluorescence switch is reproducible without obvious degradation (Figure 4c). Thus, the present beryllium complexes whose solid-state luminescence can be smoothly switched between dark and bright states by grinding/solvent annealing, acid/base vapor fuming or heating/solvent annealing provide the first example of materials with reversible triple-channel solid-state fluorescent "ON/OFF" switching properties, to the best of our knowledge.

3.3 Mechanism considerations
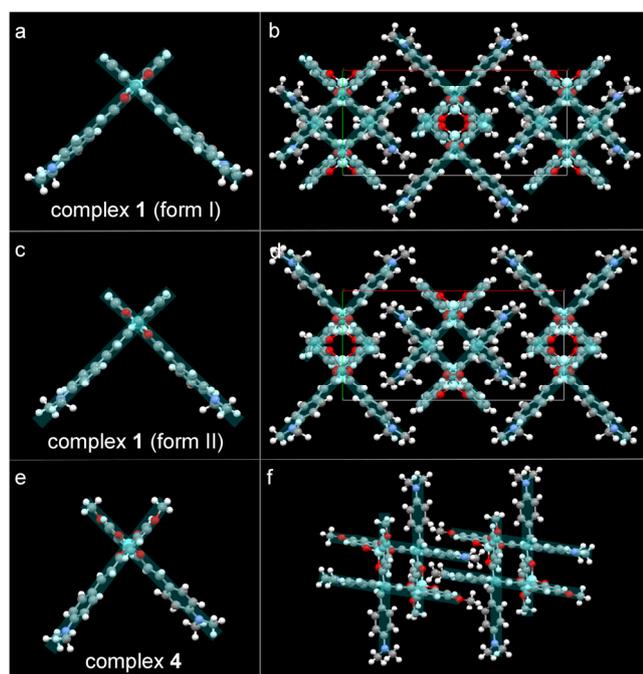
Figure 7. Cross-shape molecular structure and "#"-type stacking of crystals **1**[10] (a, b for form **I** and c, d for form **II**) and **4** (e and f).

The mechanism of the solid-state fluorescence switch by grinding/annealing processes was firstly discussed. Based on the calculation results, the two ligands of each complex are almost planar and perpendicularly fused by a beryllium atom with a dihedral angle of about 90° (Figures S8 and S10). The produced cross-shape structure facilitates molecules to arrange in a "#" manner with high molecular rigidity as well as packing stability and could avoid π-stacking in a large degree which is beneficial to the emission (Figure 8a). This packing style has been confirmed by crystal structure analyses of **1** and **4** (Figure 7). The measured PXRD patterns of the powdered complex **1** and **4** almost coincide with the simulated results from the single crystal data (Figure S9). The "#"-typed molecular packing feature may effectively restrict the photoinduced molecular distortions and eliminates the intermolecular π–electron interactions, enhancing

the emission of the crystalline samples. After grinding, the molecules transfer into a random packing mode in which the intermolecular π–π interactions may dominate and the molecules can rotate freely, resulting in a fluorescence "OFF" state.
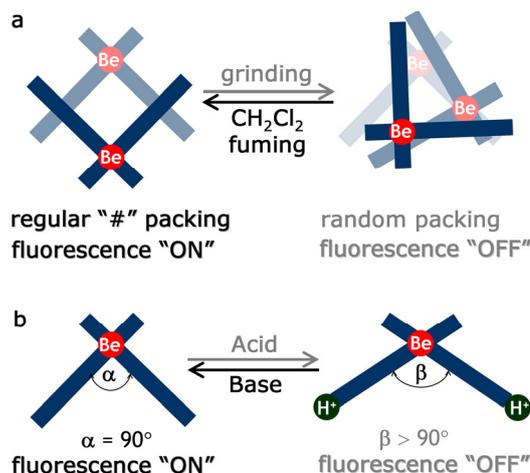
Figure 8. Molecular packing modes in the ground and fumed samples (a) and molecular conformations of neutral and acidified molecules (b).
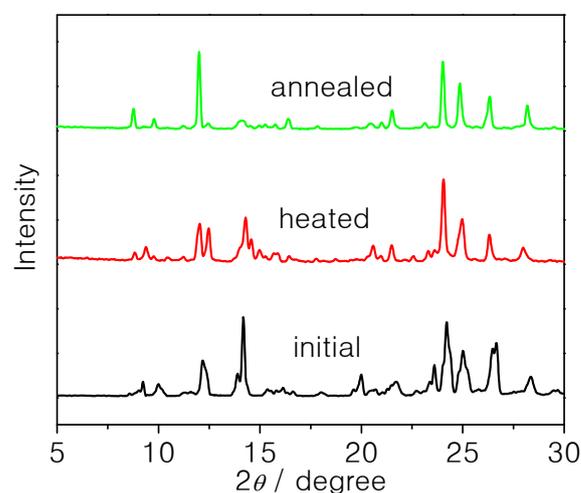
Figure 9. PXRD patterns of complex **1** in various states.

The protonation of amino groups can effectively eliminate the donor-acceptor nature and thus blue-shift the absorption and emission spectra of the complexes in the solid state. To get insights into the mechanism of the fluorescence switch of beryllium solids by acid/base vapor fuming, we optimized the molecule structure and calculated the electronic structures of the acidified species. The calculated ground and excited state geometries indicate that the structures at the protonation state occur dramatic changes with respect to their neutral state (Figure S10). The dihedral angle between two ligands in the complex is about 121° with two amino groups keeping apart from each other (Figure 8b). The distance between the two protonated nitrogen atoms is 17.6 Å, greatly larger than that (15.1 Å) of the neutral molecule. Once beryllium complex is protonated, the ligands undergo remarkable changes in planarity and shape to adapt the charge repulsion interaction. Therefore, the "#"-type packed molecules in crystalline powders might change into other packing

modes accompanied with fluorescence quenching due to the molecular conformation transformation after HCl vapor fuming.

The relationship between the heating/solvent annealing activated ON/OFF emission behavior and the molecular packing modes in the solid state was investigated by PXRD (Figure 9). The heated sample **1** shows different PXRD peaks compared to the initial crystalline solids, indicating that thermal annealing of the sample before its melt resulted in the changes in the solid-state molecular packing modes from the cross-packed manner ("ON") to another stacking architecture ("OFF") which caused fluorescence quenching to a certain degree (Figures S11–12). After cooling and solvent annealing, the solids undergo a molecular repacking process and form crystalline samples with the other cross-packing mode which make the sample to be brightly fluorescent.

4. Conclusions

In summary, we have synthesized a class of highly solid-state red/NIR emissive beryllium complexes whose emission color and intensity are directly related to the phase and morphology they adopt. Simple physical engineering processes (grinding/solvent annealing) can smoothly switch the solid-state fluorescence between dark and bright states. In addition, the Lewis-base nature of the amino groups on ligands endows the fluorescence of solids to be in response to acid vapors. Furthermore, the molecular packing modes of these complexes can be altered by heating and recovered by solvent annealing accompanied with fluorescence switching between "ON" and "OFF" states. Thus, the triple-channel fluorescence "ON/OFF" switching has been firstly realized by our group through totally different approaches (grinding/solvent annealing, acid/base vapor fuming, and heating/solvent annealing) in the solid state and this finding has scientific significance on not only creating novel fashions of fluorescence switch but also expanding applications of luminescent materials to the field of multifunctional sensing.

Acknowledgements

Notes and references

State Key Laboratory of Supramolecular Structure and Materials,College of Chemistry, Jilin University, Changchun 130012, P. R. China. Fax: (+)86-431-8519-3421; Tel: (+)86-431-8516-8496; E-mail: hongyuzhang@jlu.edu.cn

† Electronic Supplementary Information (ESI) available: [details of PL spectra, PXRD data and NMR spectra etc]. See DOI: 10.1039/b000000x/

1 Recent reviews: (a) Z. M. Hudson, S. Wang, *Acc. Chem. Res.* 2009, **42**, 1584; b) D. Li, H. Zhang, Y. Wang, *Chem. Soc. Rev.* 2013, **42**, 8416; c) Y. Hong, J. W. Y. Lam, B. Z. Tang, *Chem. Soc. Rev.* 2011, **40**, 5361; d) Z. Chi, X, Zhang, B. Xu, X. Zhou, C. Ma, Y. Zhang, S. Liu, J. Xu, *Chem. Soc. Rev.* 2012, **41**, 3878.

2 (a) Y. Kim, J. Bouffard, S. E. Kooi, T. M. Swager, *J. Am. Chem. Soc.* **2005**, **127**, 13726; (b) A. Wakamiya, K. Mori, S. Yamaguchi, *Angew. Chem. Int. Ed.* 2007, **46**, 4273; (c) A. Steffen, M. G. Tay, A. S. Batsanov, J. A. K. Howard, A. Beeby, K. Q. Vuong, X.-Z. Sun, M. W. George, T. B. Marder, *Angew. Chem. Int. Ed.* 2010, **122**, 2399; (d) J. C. Collings, A. C. Parsons, L. Porres, A. Beeby, A. S. Batsanov, J. A. K. Howard, D. P. Lydon, P. J. Low, I. J. S. Fairlamb, T. B. Marder, *Chem. Commun.* 2005, 2666; (e) V. N. Belov, M. L. Bossi, J. Fölling, V. P. Boyarskiy, S. W. Hell, *Chem. Eur. J.* 2009, **15**, 10762; (f) G. Duran-Sampedro, I. Esnal, A. R. Agarrabeitia, J. B. Prieto, L. Cerdán, I. García-Moreno, A. Costela, I. Lopez-Arbeloa, M. J. Ortiz, *Chem. Eur. J.* 2014, **20**, 2646; (g) J. Ni, X. Zhang, Y.-H. Wu, L.-Y. Zhang, Z.-N. Chen, *Chem. Eur. J.* 2011, **17**, 1171; (h) J. R. Kumpfer, S. D. Taylor, W. B. Connick, S.t J. Rowan, *J. Mater. Chem.* 2012, **22**, 14196; (i) X. Zhang, J.-Y. Wang, J. Ni, L.-Y. Zhang, Z.-N. Chen, *Inorg. Chem.* 2012, **51**, 5569; (j) J. Ni, X. Zhang, N. Qiu, Y.-H. Wu, L.-Y. Zhang, J. Zhang, Z.-N. Chen, *Inorg. Chem.* 2011, **50**, 9090.

3 (a) H. Zhang, Z. Zhang, K. Ye, J. Zhang, Y. Wang, *Adv. Mater.* 2006, **18**, 2369; (b) T. Zhou, F. Li, Y. Fan, W. Song, X. Mu, H. Zhang, Y. Wang, *Chem. Commun.* 2009, 3199; (c) Z. Zhang, Y. Zhang, D. Yao, H. Bi, I. Javed, Y. Fan, H. Zhang, Y. Wang. *Crys. Growth & Des.* 2009, **9**, 5069; (d) Z. Zhang, D. Yao, T. Zhou, H. Zhang, Y. Wang, *Chem. Commun.,* 2011, **47**, 7782; (e) C. Yuan, S. Saito, C. Camacho, S. Irle, I. Hisaki, S. Yamaguchi, *J. Am. Chem. Soc.* 2013, **135**, 8842; (f) Y. Abe, S. Karasawa, N. Koga, *Chem. Eur. J.* 2012, **18**, 15038.

4 (a) M. S. Kwon, J. Gierschner, J. Seo, S. Y. Park, *J. Mater. Chem. C* 2014, **2**, 2552; (b) J. Liang, Z. Chen, L. Xu, J. Wang, J. Yin, G.-A. Yu, Z.-N. Chen, S. H. Liu, *J. Mater. Chem. C* 2014, **2**, 2243; (c) X. Y. Shen, Y. J. Wang, E. Zhao, W. Z. Yuan, Y. Liu, P. Lu, A. Qin, Y. Ma, J. Z. Sun, B. Z. Tang, *J. Phys. Chem. C,* 2013, **117**, 7334.

5 (a) H. Bi, D. Chen, D. Li, D. Xia, Z. Zhang, H. Zhang, Y. Wang, **Chem**. *Commun.,* 2011, **47**, 4135; (b) W. Liu, Y. Wang, M. Sun, D. Zhang, M. Zheng, W. Yang, *Chem. Commun.,* 2013, **49**, 6042; (c) J. Zhang, J. Chen, B. Xu, L. Wang, S. Ma, Y. Dong, B. Li, L. Ye, W. Tian, *Chem. Commun.,* 2013, **49**, 3878.

6 (a) C. Li, Y. Zhang, J. Hu, J. Cheng, S. Liu, *Angew. Chem. Int. Ed.,* 2010, **49**, 5120; (b) Y. Kim, H.-Y. Jung, Y. H. Choe, C. Lee, S.-K. Ko, S. Koun, Y. Choi, B. H. Chung, B. C. Park, T.-L. Huh, I. Shin, E. Kim, *Angew. Chem. Int. Ed.,* 2012, **51**, 2878; (c)H. Kobayashi, P. L. Choyke, *Acc. Chem. Res.,* 2011, **44**, 83; (d) P. Audebert, F. Miomandre, *Chem. Sci.,* 2013, **4**, 575.

7 (a) C. Li, X. Luo, W. Zhao, C. Li, Z. Liu, Z. Bo, Y. Dong, Y. Q. Dong, B. Z. Tang, *New. J. Chem.,* 2013, **37**, 1696; (b) C. Dou, L. Han, S. Zhao, H. Zhang, Y. Wang, *J. Phys. Chem. Lett.,* 2011, **2**, 666; (c) D. Liu, Z. Zhang, H. Zhang, Y. Wang, *Chem. Commun.,* 2013, **49,** 10001; (d) K. Wang, S. Huang, Y. Zhang, H. Zhang, Y. Wang, *Chem. Sci.,* 2013, **4**, 3288; (e) Z. Ma, M. Teng, Z. Wang, S. Yang, X. Jia, *Angew. Chem. Int. Ed.,* 2013, **52**, 12268; (f) Y. Dong, B. Xu, J. Zhang, X. Tan, L. Wang, J. Chen, H. Lv, S. Wen, B. Li, L. Ye, B. Zou, W. Tian. *Angew. Chem. Int. Ed.*, 2012, **51**, 10782; (g) K. Nagura, S. Saito, H. Yusa, H. Yamawaki, H. Fujihisa, H. Sato, Y. Shimoikeda, S. Yamaguchi, *J. Am. Chem. Soc.,* 2013, **135**, 10322.

8 (a) T. Han, J. W. Y. Lam, N. Zhao, M. Gao, Z. Yang, E. Zhao, Y. Dong, B. Z. Tang, *Chem. Commun.,* 2013, **49**, 4848; (b) H. Gu, L. Bi, Y. Fu, N. Wang, S. Liu, Z. Tang, *Chem. Sci.,* 2013, **4**, 4371; (c) R. Rao M, C.-W. Liao, W.-L. Su, S.-S. Sun, *J. Mater, Chem. C,* **2013**, **1**, 5491; (d) Y. Zhang, J. Sun, G. Zhuang, M. Ouyang, Z. Yu, F. Cao, G. Pan, P. Tang, C. Zhang, Y. Ma, *J. Mater. Chem. C,* 2014, **2**, 195 (e) J. W. Chung, S.-J. Yoon, B.-K. An, S. Y. Park, *J. Phys. Chem. C,* 2013, **117**, 11285.

9 (a) X. Cheng, H. Zhang, K. Ye, H. Zhang, Y. Wang, *J. Mater. Chem. C,* 2013, **1**, 7507; (b) X. Cheng, D. Li, Z. Zhang, H. Zhang, Y. Wang. *Org. Lett.,* 2014, **16**, 880.

10 Y. Dong, J. W. Y. Lam, A. Qin, Z. Li, J. Sun, H. H.-Y. Sung, I. D. Williams, B. Z. Tang, *Chem. Commun.*, 2007, 40.

Graphical Abstract
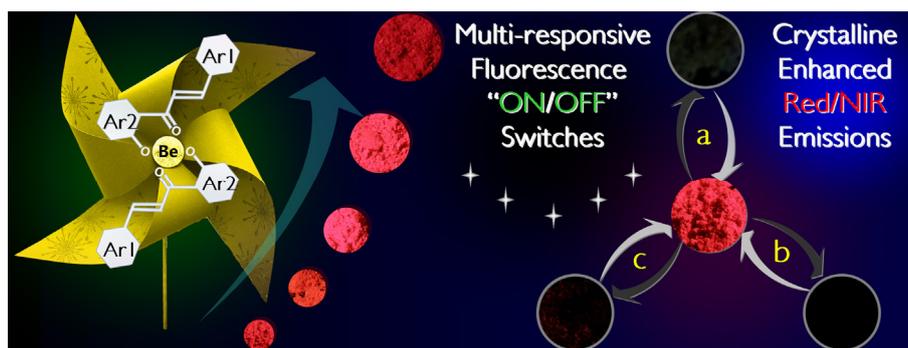
Crystalline-enhanced red/NIR emission of beryllium complexes can be switched between dark and bright states by different stimuli, providing the first example of reversible multiple-channel solid-state fluorescent "ON/OFF" switching.